



Development of a 0.25 m f/10 reflecting telescope consisting of a thin primary mirror and a friction drive

H.S.D. Amaradasa, K.G. Samarathna, S.S. Abeywickrama, E.M. Ranatunga and G.D.K. Mahanama*

Department of Physics, University of Ruhuna, Matara, Sri Lanka

* Correspondence: mahanama@phy.ruh.ac.lk;  <https://orcid.org/0000-0002-4761-4558>

Received: 27th March 2019, Revised: 12th March 2020, Accepted: 28th June 2020

Abstract Modern astronomical telescopes are comprised of high-quality optics and superior mounting designs to meet the standards and challenges of observational astronomy. Cost of commercial telescopes is a constraint for developing countries like Sri Lanka to be involved in astronomical related research. The objective of this research was to study the technological methods used in fabricating telescopes and to implement those methods to make economical telescopes locally. Therefore, a f/10 focal ratio Newtonian telescope consisting of a computerized friction drive alt-azimuth mount was fabricated with a locally ground thin telescope primary mirror made from Soda-lime glass plate having 0.25 m diameter and 0.012 m thickness. Deformation characteristics, profile formation and optical performance of the telescope primary mirror were investigated using finite element analysis, Polarization and Ronchi pattern analyses, respectively. Resolution, slew rate, torque and slippage of the fabricated friction drive were studied using a Computer Aided Design (CAD) model and an empirical approach. It was found that the profile of the mirror is a perfect parabola. The mirror was supported by a mirror cell with eighteen floating points and resultant root mean square wave-front error of the mirror due to the supporting points is 3.735×10^{-7} m. The friction drive with the computer controller can position the telescope to a given angle with accuracies of 0.421 degrees on altitude axis and 0.03 degrees on azimuth axis. The total cost of production of the prototype telescope is about US\$ 750.00. It is shown that there is a significant cost reduction and increased optical and mechanical performances of the telescope due to using the thin mirror and the friction drive mount. In this paper, the system design and the performance evaluation of the mechanical positioning and optical quality of the telescope are presented.

Keywords: Newtonian telescope, mirror grinding, telescope driving system, thin telescope mirror.

1 Introduction

Use of small aperture (0.2-1.0 m) automated telescopes have increased substantially during the past two decades. Las Cumbres Observatories, Stellar Oscillations Network Group (SONG) (Grundahl *et al.* 2008), International Scientific Optical Network



(ISON) (Schmalz *et al.* 2019), Hungarian-made Automated Telescope Network (HATNet) (Bakos *et al.* 2002) and iTelescope network have used automated small telescopes for impactful research in the fields of Photometry, Near-Earth object detection, spectrometry and transient detection (Henry and Eaton 1995). The fabrication cost of telescopes has significantly decreased due to the invention of thin telescope mirrors and computerized alt-azimuth mount (Cheng 2009). However, the design and fabrication of cost-effective astronomical telescopes incorporates unique technological challenges.

The primary mirror fabricated in this work has a parabolic profile. Conventionally, parabolic primary mirrors are made using thick glass plates (Genet *et al.* 2009) with thickness to diameter ratio greater than 1/6. Mirrors of thickness to diameter ratio less than 1/6 are considered as thin mirrors (Genet *et al.* 2009). Therefore, a mirror of a diameter 0.25 m should comprise of minimum thickness of 0.041 m. A thick glass may decrease warping of the glass plate during grinding and minimize deformation of the curvature of the mirror when fixing in the telescope mount (Luc 1995). In most cases a substantial proportion of the weight of a telescope is due to the mass of the primary mirror. Hence, reduction of the mirror thickness is an important factor in a telescope design. Thin mirror allows reduction in weight thereby reducing the weight and consequently the cost of the instrument. In this research a 0.25 m diameter f/10 parabolic telescope mirror was fabricated from 0.012 m thickness glass plate. Subsequently a mirror cell, optical tube and a computerized driving system were made to match the optical parameters of the fabricated mirror. An attempt to fabricate a telescope has improved the knowledge and tools required for developing the technology. In addition, the final product can be used as an educational tool in universities and schools (Gebhardt *et al.* 2017). Hence, the main objective of this research project was to study the technological methods for fabricating economical telescope for Sri Lanka.

2 Material and Methods

2.1 Fabrication of the primary mirror

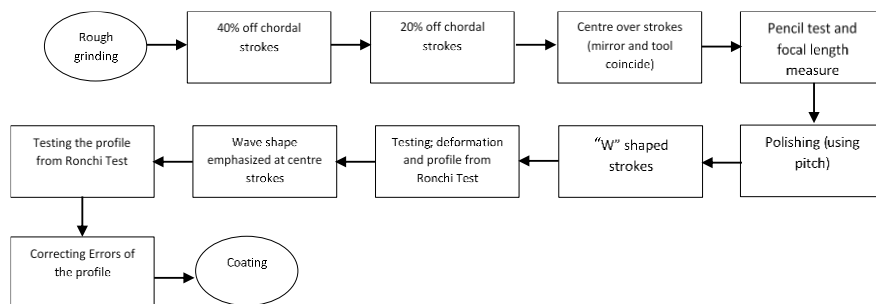
The surface profile accuracy of the primary mirror should be less than $\frac{1}{4}$ wavelength of light (Malacara 2007). Therefore, the primary mirrors are made using an intricate process of grinding and polishing to make a uniform concave shape. In addition, the primary mirror substrate materials must have specific properties such as a low coefficient of thermal expansion, higher hardness, higher thermal conductivity, and low specific heat capacity (Cheng 2009). Hence, an ideal primary mirror may inherit a stable surface profile over a long period, minimum deformation due to temperature variations, rigidity to sustain stress induced during fabrication and an ability to coat in a high vacuum ($\sim 10^{-5}$ mbar). The materials mainly used in this purpose are Pyrex (material code 7740), Fused Silica (Quartz), Plate Glass (Soda-lime), BK-7, Astrositall, Zerodur, Cer-Vit, SiC, metals and alloys (Cheng 2009). Out of these, plate glass is a

cost-effective material which is available in the local market. The plate glass has a density of 2.5 g/cm^3 , 73 GPa Young's modulus, 470 Knoop hardness, $8.6 \times 10^{-6} \text{ }^\circ\text{C}^{-1}$ coefficient of thermal expansion, $0.75 \text{ W/m }^\circ\text{C}$ thermal conductivity and $0.7 \text{ kJ/kg }^\circ\text{C}$ specific heat capacity (Scholze 1991). In this research, a 12 mm thick plate glass blank was used to make the telescope mirror.

The primary mirror with 0.25 m aperture and 2.5 m focal length (f/10) was fabricated by grinding off glass from the flat blank. Two identical disks were cut using plate glass (Soda-lime) for producing two blanks. One disk was used as the tool and the other as the mirror. One side of a glass disk (one selected for the mirror) was ground to the parabolic concave shape using Silicon Carbide (SiC) and Aluminium Oxide (Al_2O_3) abrasives of different grit sizes. Uniformity of the grinding process was checked at various stages. Ferric Oxide (Fe_2O_3) and Optical pitch were used in the polishing process (Wilson 1999). Mirror profile was checked using a parallel beam of light (Wilson 1999). Profile shape was analysed using the Ronchi test (Malacara 2007). Deviations from the required parabola profile were identified by comparing with the standard Ronchi images.

Grinding process

Rough grinding, fine grinding, polishing and testing are the main phases of the grinding process. The rough grinding is the phase where initial profile is made, typically using abrasives 60-1000 grit sizes and 12, 5 and 3-micron sizes. The rough grinding was performed by fixing the tool disk on a horizontally rotating surface. A paste of water and Silicon Carbide (SiC) was poured on the tool surface. With the mirror disk on top, the mirror was moved radially sideways about 40% of its diameter over the tool making most of the grinding actions at the centre of the mirror and at the edge of the tool. Straight strokes were applied such that the centre of the mirror travels along a Chordal fashion (Richard B 1985). After twenty Chordal strokes, the mirror and the tool were rotated 45 degrees to opposite directions and the process was repeated with replenishing the abrasive paste (Flow Chart 1). The procedure was followed until the mirror reach the required focal length. The sagitta of the mirror profile was checked after each hour of grinding.



Flow Chart 1: Grinding process followed in the 0.25m f/10 mirror formation

Polishing and testing

The Pencil test was used to determine the contact between the mirror and the tool during the grinding process (Malacara 2007). In this test a radial grid pattern was drawn on to the surface of the mirror using a pencil. Pencil marks were disappeared with normal storks. The close contacts between the mirror and the tool was deduced by watching the rate disappearing of pencil marks across the mirror. During polishing phase the grinding procedure was repeated by decreasing the particle size of the abrasives from 80, 120, 220, 500 and 1000 grit sizes, respectively. Fine polishing was started with 12-micron Aluminium Oxide (Al_2O_3) making centre over centre strokes and continued with 5 and 3-microns Al_2O_3 , consecutively. Ferric Oxide (Fe_2O_3) and an Optical pitch (a natural resin) were also used in the polishing process (Wilson RN 1999). Table 1 illustrates the time periods spent in each grinding step with abrasives and polishing.

Table 1: Grinding and polishing times for the 25 cm diameter, 0.012 m thick glass for obtaining a focal length of 2.5 m

Abrasive, grain size	Grinding Time
SiC 60 grit	20 hours
SiC 80 grit	10 hours
SiC 120 grit	6 hours
SiC 220 grit	4 hours
SiC 500 grit	4 hours
SiC 1000 grit	2 hours
Al_2O_3 1400 grit	2 hours
Al_2O_3 4500 grit	2 hours
Al_2O_3 8000 grit	20 minutes
Polishing	2 hours

The rough grinding created a spherical surface and during the polishing process the spherical surface was converted into the required paraboloid profile (Richard 1985). A lap made of Optical Pitch was used as the tool and the tool was moulded utilizing the glass tool as the base. Square grooves were cut in the surface of the lap. The polishing is a chemical-mechanical process (Cheng 2009) where micro-facets are created in the surface to increase the area of reaction. In the initial polishing, spherical profile obtained in the rough grinding was further polished. W shaped-Strokes (Howard 1984) were done to polish the spherical surface by placing the lap over the mirror. Fe_2O_3 powder which reacts with the Pitch in such a way that the surface of the glass liquefies to fill the minuscule facets on the surface was used for polishing (Hasanuzzaman and Olabi 2016). Subsequently, the Ronchi test was done to check the spherical profile. Deformation caused during the grinding at this stage was analysed using the interferometric pattern forms in the Ronchi test by checking the changes with time due to deformation of telescope mirror (Malacara 2007). Then the edges of the Pitch lap were trimmed in such a way that the lap has more contact area in the middle. The wave shaped strokes were carried out to create the paraboloid shape of the mirror. The

Ronchi test was carried out after each polishing session which indicated the formation of the profile (paraboloid). The telescope mirror needed to be coated with a thin Aluminium (Al) layer inside a vacuum coating system (Wilson 1999). This facility was not available in Sri Lanka. Therefore, the completed telescope mirror was sent to the National Astronomical Research Institute of Thailand and Al reflective layer was coated using thermal evaporation. The completed telescope mirror was tested by attaching to a prototype telescope mount for observing ground objects and creators on the moon.

A mirror cell dimensions varies with diameter, thickness and focal length of the mirror (Luc 1995). Positions and number of supports required were calculated using a Plate Optimizing (PLOP) software. The software uses finite element analysis to map the deformation of the telescope primary mirror. Mirror cell topology used in this research is consisted of multiple support locations all with free-floating joints (Figure 1).

Floating support for the primary mirrors

Traditionally, telescope primary mirrors have a diameter/thickness ratio (aspect ratio) less than 6 (Burge 1993). However, recently developed large monolithic mirror telescopes have aspect ratios much larger than 20 (Mueller *et al.* 1993) and segmented mirror telescopes have aspect ratios as large as 110 (Smith 1989). Tendency to deform a thin mirror (aspect ratio > 6) is greater, especially during the grinding phase and during installation process of the telescope mirror. In the grinding process, a large force applied to the mirror may cause the mirror blank to bend. Therefore, the manufactured profile of the mirror may change over time (Nelson *et al.* 1982). In a worst-case scenario, the mirror blank may permanently deform.

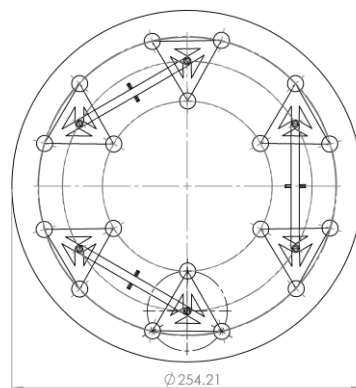


Fig.1: Schematic diagram of the eighteen-point floating support

In the installation process, gravitational loading and force applied from the mirror cell could introduce surface deformations. Therefore, special mirror supporting systems

with an increased number of supporting points are required to support thin mirrors (Jingquan and Humphries 1982). There are two types of mirror support systems namely positioning and floating. In the positioning system, the mirror is fixed (using adhesives) to static support points. The floating supports also known as astatic flotation and all the supporting points of this design are dynamic. Therefore, the reaction exerted on the mirror mimics a buoyant force created from liquid (Cheng 2009). In this design eighteen-point floating support system was utilized to minimize the deformation of the thin mirror. The schematic diagram the system is shown in Figure 1.

The polished mirror is tested using the Ronchi test where interferometric patterns reveal permanent and temporary deformations. Polarization test (Malacara 2007) was carried out to photograph the residual stress build up in the material. The deformation caused by residual stress will deviate the mirror profile from the required paraboloid curve. Special polishing process can correct most of the distortions but some of the severe distortions cannot not be corrected. Therefore, the conventional grinding process was modified to minimize the deformation in the study. In conventional mirror grinding procedure, weight of 2-3 kg is placed on the mirror to press the mirror against the tool (Richard 1985). In addition, manual pressure is exerted to increase glass wearing off. Extra grinding time had to be consumed due to the usage of lower pressure exerted upon the mirror. To decrease the accumulation of deformations during the grinding process the mirror was submerged in a hot water bath (373 K) after each grinding phase. The mirror was left to cool down for three to four days in the open air to relive accumulated stress before switching to the next grinding phase. Hence, glass will not create further distortions while the rest of the grinding process for the required profile.

2.2 Telescope mount

Design

The telescope system is comprised of optical tube holders, electrical system, tracking and controlling units. Pointing the optical tube with great accuracy and providing structure to stabilize the telescope are some of the concerns of system design (Gupta 1996). The telescope mounts can be categorized into two configurations, (a) Equatorial and (b) Altitude-Azimuth (alt-azimuth) (Willstrop 1995). The German-equatorial mount, which is a sub configuration of the equatorial mount has been used widely in small telescopes. The mechanical design of German-Equatorial mount has three independent rotational axes namely polar, right ascension (RA) and declination (DEC) (Cheng 2009). However, the alt-azimuth mount has only two independent axes. Hence, the performance of the alt-azimuth telescope mount rivals other designs in sturdiness, compensate torsion, minimum bending of the optical tube and storage ability (Cheng 2009). In addition, alt-azimuth design simplifies the issues related to cost and fabrication complexity. Thereby, an alt-azimuth mount design was selected for the telescope made in this research due to the considerable heavy weight (25 kg) of the telescope design.

Friction drive

Driving system of a telescope mount composed of a mechanical, electrical and software units. Worm gear, spur gear, belt, chain, direct and friction drive are some of the mechanisms used in telescope drive systems (Guo-min 2017). Friction drivers are the mechanisms that use direct power transfer to the load instead of using a chain and sprockets (Rodriguez *et al.* 2017). The friction drive mechanism has been used successfully in recently developed large telescopes such as Magellan Telescope (Gunnels and Carr 1994) and Large Sky Area Multi-Object Fibre Spectroscopic Telescope (LAMOST) (Wang *et al.* 2004). Therefore, in this research, a friction drive system was adopted. However, the friction drive mechanism has its drawbacks such as creeping and backlash (Wang *et al.* 2008). Thereby a feedback control system was implemented with the mount to minimise these drawbacks.

Encoders and feedback

One of the main drawbacks of a friction drive system is the slippage. Therefore, feedback methods consist of rotation sensors and angular encoders have been used intensively in telescope mounts with frictional drive systems (Rodriguez *et al.* 2017). The rotational sensors and angular encoders indicate the precise position of the optical tube, show up backlash and mechanical hysteresis effects in the mounting (Van Breda and Culshaw 1990). The outputs from the encoders are used in determining the position errors in the mechanical driving system quantitatively and then feedback this error to the control system (Wang *et al.* 2008). Different encoders such as optical encoders, grating tapes, inductosyns and gyroscopes have been used for this purpose (Cheng 2009). In recent telescope mount designs mechanical, optical and digital gyroscope sensors are tested for increasing the accuracy of the pointing mechanism (Tripurari and Ravi 2013). In this research, two digital accelerometers and gyroscopes were utilized with optical encoders to measure the positions and correct the pointing errors of the mount.

Design and analysis of telescope mount system

Initially, a model of Dobsonian mount was created in CAD and the rotational inertia, torque and angular acceleration of the optical tube generated in the system were calculated. Moment of inertia around both altitude and azimuth axes were also calculated. The moment of inertia varies from the horizontal position to zenith position. It is assumed that the total mass of the telescope is spread evenly in a cylinder when the telescope is pointed at the zenith for the azimuth axis. The torque required to rotate the telescope in both altitude and azimuth axes was also calculated.

Slew rate is the controlled angular motion when the telescope moves to a given position (Laing 1995). The telescope mounts are equipped with different levels of slew rates. Angular acceleration of the telescope must be determined considering the fastest slew rate required. For medium-sized telescopes, generally used fastest slew rate is 90° rotation within 30 seconds (Laing 1995). Within this slew rate the telescope should be

accelerated up to the midpoint and decelerated to the destination when moving to a given destination. Therefore, torque and the angular acceleration of the system were calculated using equations (1), (2) and (3),

$$\tau = I\alpha \dots \dots \dots (1)$$

$$\theta = \omega_0 t + \frac{1}{2} \alpha t^2 \dots \dots \dots (2)$$

$$\alpha = \frac{4\theta}{t^2} \dots \dots \dots (3)$$

where, θ - angular displacement of the optical tube of the telescope
 ω_0 - initial rotational velocity (zero)
 t - elapsed time
 α - angular acceleration

2.3 Prototype

The first prototype was fabricated using mostly wood. It was evident that the friction in the system was greater in such a way that motor driving system was less effective. The friction had to be reduced for enabling motors to drive the two axes of the telescope. Therefore, a second mount was designed by minimizing the errors in the first prototype. Stainless steel, Aluminium, plywood and plastic materials were used to fabricate the components of the second mount. The telescope design consists of a primary cage, secondary cage and truss tubes. The primary cage was made of stainless steel. Here, the octagonal shaped secondary cage was made using Aluminium box bars, waterproof opaque tent canvas material and thin Aluminium straps. The weight of the secondary cage was decreased to minimize the moment of inertia of the telescope in the altitude axis. Eight Aluminium truss tubes were used to connect the primary and secondary cages. The primary and secondary cages were connected from the lightweight frame which further minimized the moment of inertia. A 3.5 cm diameter, flat, diagonalized, Aluminium coated mirror was used as the secondary mirror. A base plate is supporting the entire weight of the telescope and this base plate is supported by three caster wheels for rotating the telescope in azimuth axis.

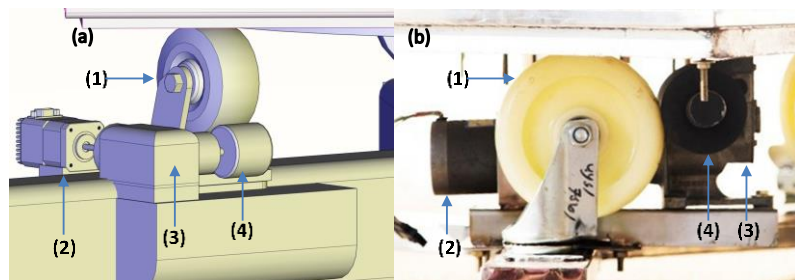


Fig. 2: Images of Azimuth driving system, (a) the CAD model and (b) the actual implementation
 (1: the castor wheel, 2: motor, 3: gear box, 4: actuator).

Two stepper motors and worm gearboxes were used to drive the telescope on both altitude and azimuth axes. In the altitude axis, a worm gear box was connected to the semicircle wheel (Figure 2). In the azimuth axis the second worm gear box was connected to a caster wheel (Figure 3).

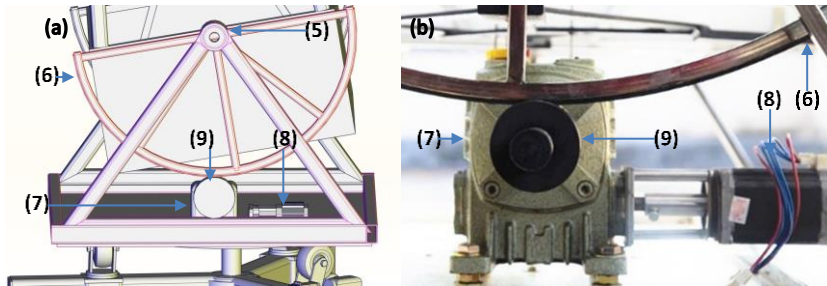


Fig. 3: Images of Altitude driving system, (a) the CAD design with the main pivoting point, and (b) the fabricated unit (5: altitude pivot point, 6: semi-circle wheel, 7: gearbox, 8: the motor, 9: actuator).

A Raspberry Pi 3 Single Board Computer (SBC) was used as the processing unit of the telescope movement control. The SBC was programmed to drive the altitude and azimuth motors, measuring the orientation of the optical tube, and remotely controlling the telescope. To control the telescope remotely, the SBC was connected to a wireless network in such a way that any computer in the local network can access the SBC through a command line interface such as PuTTY (www.putty.org). For accessing the telescope via internet, a virtual private network (VPN) was configured. This gives entire control of the SBC to a remote user (Caldas-Calle *et al.* 2017).

Generally, a remote telescope requires a star catalogue to identify RA and DEC of stellar objects (Melsheimer and Genet 1984). An open source software named Stellarium (www.stellarium.org) has been used in several similar studies for controlling the orientation of the optical tube of telescopes (Cheng *et al.* 2011). Therefore, here Stellarium was used in the SBC as the star catalogue. A hardware named “A4988” stepper motor drive carrier and a firmware were used to connect the SBC with the motors. An MPU 6050 and Rotary encoders were used to detect the direction of the optical tube. One accelerometer-gyroscope sensor was positioned at the upper cage of the telescope and the other one is placed at the lower part of the telescope for measuring the acceleration of the optical tube and the lower cage, respectively.

3 Results & Discussion

3.1 Test results of the thin telescope mirror

Figure 4 shows (a) the top view of the completed mirror, (b) the completed mirror cell in accordance with the calculated values, and (c) the mirror attached to the floating

points using silicon adhesives. During observations it was evident that the mirror cell holds the mirror steadily while the optical tube of the telescope is in horizontal and vertical positions.

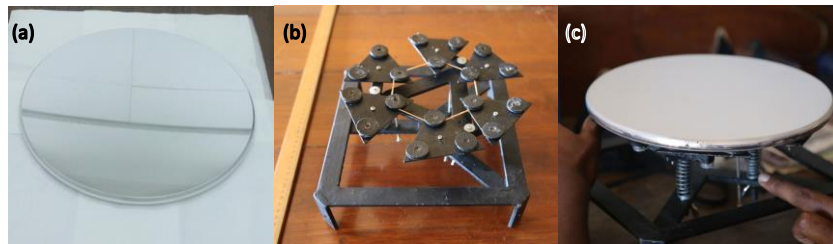


Fig. 4: (a) Top view of the coated mirror, (b) completed mirror cell and (c) side view of the mirror attached to the mirror cell.

Results of the Polarization test indicated that the glass blanks used for the mirror and tool had no accumulated stress prior to the grinding. Since the glass blanks selected here were thin, it was expected to see accumulation of stress during the grinding process. However, polarization test done after rough grinding did not indicate any stress accumulated in the primary. This proves that the glass material, thickness of the primary and the grinding procedure selected in the research is successful on mitigating stress. Results of Ronchi test revealed that the curvature around the edge of the primary mirror is defective. The defect was identified as the turned-up edges. However, the observed Ronchi pattern indicated a uniform spherical curvature after additional polishing time concentrated around the edges. The final Ronchi test was done after the parabolization process. This indicated a pattern which resembles a uniform curvature, from edge to the centre of the primary mirror (Figure 5).

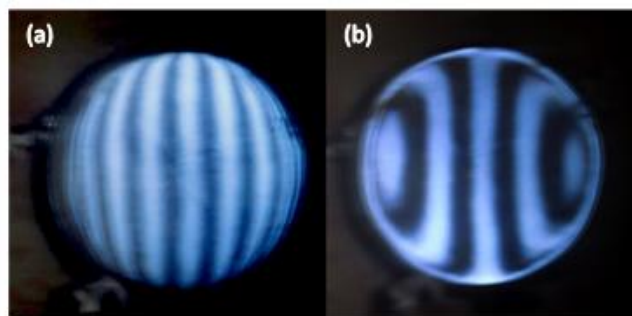


Fig. 5: (a) view of the Ronchi pattern observed at 10.2 mm inside the radius of curvature and (b) observed pattern at 10.2 mm outside the radius of curvature.

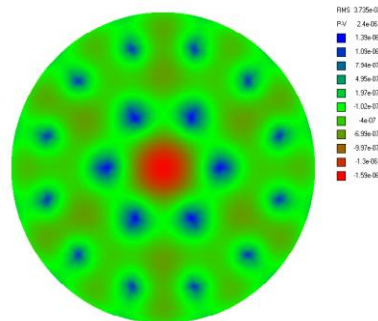


Chart 2: Surface deformation colour plot generated from the PLOP

The calculation of mirror cell support points indicated that mirror needed to be supported in eighteen floating points. Graphical output of the calculation is illustrated in the colour plot (Chart 2). The colour plot predicts resultant bending causes by the eighteen floating point axial supports. Peak-Valley (PV) difference expected in the surface of the mirror is indicated in the blue-red gradient where a depression is indicated in red. Here, the maximum peak is 1.39×10^{-6} m which is at the supporting points. A valley of 1.59×10^{-6} m is formed at the centre of the mirror. The centre of the mirror is obstructed by the secondary mirror. Therefore, deformation formed at the centre will have less effect on overall optical performance of the mirror. Hence, it was evident that the mirror cell design helps to maintain Root Mean Square (RMS) error of the mirror in a tolerable value of 3.75×10^{-7} m.

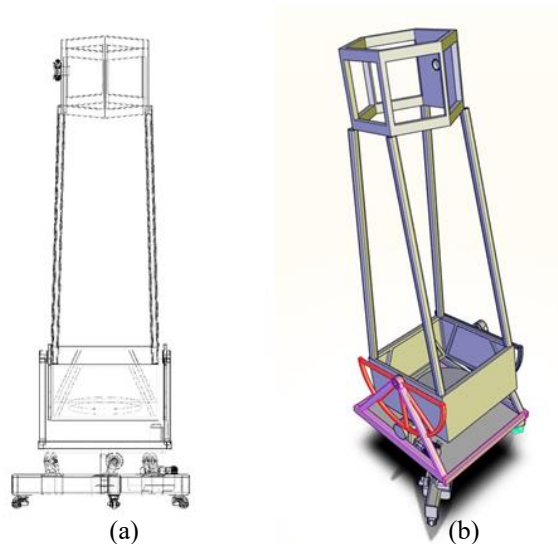


Fig. 6: CAD design of the overall telescope; (a) front view of the technical drawing and (b) the isometric view

3.2 Results of the telescope mount development

Figure 6 shows the finalized CAD design of the telescope, (a) the front view of the technical drawing and, (b) the isometric view. According to the CAD design, the weight of the entire telescope is distributed upon three caster wheels (item 1 labelled in Figure 2). The motor driving mechanism is attached to one of the caster wheels where a small platform houses the gear wheels and the motor. The altitude axis was driven using the semi-circle metal frame (item 6 labelled in Figure 3) in the telescope where a rubber wheel attached to the second worm gear. The weight of the telescope tube is pivoted around the main pivoting point in such a way that torque exerted in the semi-circle wheel is minimized. Therefore, the motor is subjected to less torque depending on the dimensions of the CAD model the telescope was made.

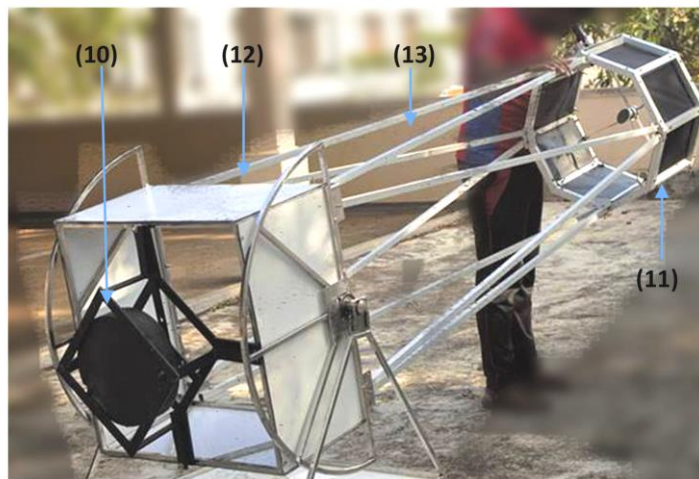


Fig. 7: Photograph of the manufactured prototype telescope

The final version of the manufactured prototype telescope shown in Figure 7. It consists of the upper cage (11), the lower cage (12) and four truss-tubes (13). The primary cage rotates 0.421 degrees around the azimuth axis for a single step of the stepper motor according to the calculations. The primary cage rotates 0.03 degrees around altitude axis for a single step of the stepper motor. According to the readings of the gyro-accelerometer and encoder sensors the telescope functions as planned up to an altitude angle of 40° from the zenithal axis. However, it was found that in lower angles ($<40^\circ$) the driving system experiences slippage and unnecessary vibrations. The cause of this has been identified as the displacement of the centre of gravity of the optical tube with the altitude angle. Hence, the centre of gravity of the optical tube was conveyed to a lower position than the original. This was achieved by placing a 26.5 kg counter weight (item 10 in Figure 7) under the mirror cell.

The incorporation of the SBC allowed to remotely point the telescope and read the feed-back from gyro-accelerometer sensors. However, a delay associated with the remote operation was identified. The actual pointing direction of the telescope was updated in the Stellarium interface after 10-20 seconds. It was found that the delay was originated in the motor driving hardware and SBC communication. Despite the delay the telescope can be pointed to a given RA and DEC accurately. Since, the view of the telescope is not obtained, an astronomy camera was integrated with the telescope. It is expected to compare real time view with the RA and DEC pointed in the driving mechanism. Specifications of the manufactured telescope is given in Table 2.

Table 2: Characteristics of the manufactured prototype telescope.

Properties	Value
Primary mirror	
Diameter (physical)	258 mm
Diameter (optical)	251 mm
Radius of curvature	5.1 m
Focal ratio	10.159
Sagitta	1.564 mm
Angular Resolution	0.451 arcsec
Limiting Magnitude	15.9 Mag
Coating	99 % Al
Secondary mirror	
Diameter	35.50 mm
Obstruction	2.38 %
Spacing	
Primary-secondary space	2434.0 mm
Focuser tube distance	76.3 mm

4 Conclusions

In this paper, we proposed a simplified telescope making technique which can be used to fabricate cost-effective automated telescopes. A Newtonian mirror of diameter 0.25 m focal length of 2.5 m (f/10) and thickness of 0.012 m was fabricated utilizing the conventional mirror grinding procedures. The primary mirror was made using a thin locally available glass material. Single board computer which is a new automation technology was incorporated to allow remote operation. The curvature of the mirror was tested using the Ronchi test and results indicated a uniform curvature with minimum deformations. Gravitational loading of the mirror was calculated and the axial support which can counteract the gravitational loading was made using estimations generated by PLOP analysis. Combination of thin mirror and the mirror cell enables to produce lightweight economical telescope mirror beyond the general limitations in the diameter and thickness. The optical design of this telescope has high magnifying power, resulting magnification of 208 for a 12 mm eyepiece. A Raspberry Pi 3 single board computer was integrated with the telescope for controlling and

obtaining the input from sensors. It was found that the oscillation of the telescope tube due to the wind is infinitesimal. This is due to the greater inertia of the telescope and friction of the gear reduction system. The telescope driving system developed in this research can drive the telescope in both Altitude and Azimuth axes. A worm gear reduction system was used with two 1.8-degree stepper motors. The completed system can position the telescope to a given angle with the accuracies of 0.421 degrees on the azimuth axis and 0.03 degrees on the altitude axis. The total spent to produce the prototype telescope was approximately US\$750. The optical quality of the prototype telescope, tested observing ground objects, has shown satisfactory functioning. Observation of the moon shown clear pictures of the craters on the moon surface. It should be noted that this is the first attempt of making a workable telescope in Sri Lanka using local expertise, local material, and local technology. Since manufacturing the first prototype, authors now have developed the facility for Aluminium coating of glass enabling the commercialization of telescope manufacturing in Sri Lanka with further reduced cost.

Acknowledgements

The authors acknowledge the financial support received from The University of Ruhuna, Faculty of Science Research Grants (RU/SF/RP/2014/04 and SF/RG/2016/08), the National Research Council (NRC) Grant NRC 16-01 and also the equipment grant (NSF/RG/2015/EQ/10) from the National Science Foundation of Sri Lanka. Further, the authors are thankful to Prof. B. Soonthornthum, Mr. S. Aukkaravittayapun and Mr. A. Leckngam of National Aeronautical Research Institute of Thailand for mirror fabrication. Especially thankful to the anonymous reviewers whose constructive comments and critical review improved the quality of the manuscript.

References

- Bakos GA, Lazer J, Papp I, Sari P, Green EM. 2002. System description and First Light Curves of the Hungarian automated telescope, an autonomous observatory for variability search. *Publications of the Astronomical Society of the Pacific* 114 (799): 974-987.
- Burge JH. 1993. Advanced Techniques for Measuring Primary Mirrors for Astronomical Telescopes. Ph.D. Dissertation. Optical Sciences. University of Arizona. pp 140-146.
- Caldas-Calle L, Jara J, Huerta M, Gallegos P. 2017. QoS evaluation of VPN in a Raspberry Pi devices over wireless network. *International Caribbean Conference on Devices, Circuits, and Systems: [proceedings]*. pp 125-128.
- Chen J, Meng L, Wang X, Wang C. 2011. An integrated system for astronomical telescope based on stellarium. *3rd International Conference on Advanced Computer Control*. pp 431-434.
- Cheng J. 2009. Mirror Design for Optical Telescopes. *The Principles of Astronomical Telescope Design* 360: 87-139.
- Gebhardt, P, Schrimpf A, Dersch C, Spasovic M, Bringmann L, Singh HP, Gupta R, Kanbur SM. 2019. U-SMART: Small aperture robotic telescopes for universities. *Revista Mexicana de Astronomiay Astrofisica: Serie de Conferencias*. pp. 44-46.
- Genet R, Aurigema A, Badger S, Bartels M, Brodhacker KL, Canestrari R, Chen P, Connelley M, Davis D, Ghigo M, Jones G, Liu T, Mendez E, Pareschi G, Richardson T, Rowe R, Schmidt J, Shah K,

- Villasenor E. 2009. Lightweight Mirror Developments. Proceedings for the 28th Annual Symposium on Telescope Science. Society for Astronomical Sciences. pp 28-33.
- Grundahl F, Arentoft T, Christensen-Dalsgaard J, Frandsen S, Kjeldsen H, Rasmussen PK. 2008. Stellar Oscillations Network Group – SONG. *Journal of Physics: Conference Series*. 118(1): 20-22.
- Gunnels SM, Carr D. 1994. Design of the Magellan Project 6.5-meter telescope: telescope structure and mechanical systems. *Advanced Technology Optical Telescopes 2199*: 414–427.
- Guo-min, WANG. 2017. Review of Drive Style for Astronomical Optical Telescope. *Progress in Astronomy*. 25(4): 374-382.
- Gupta R. 1996. Small telescopes and robotics. *Bulletin of the Astronomical Society of India* 24: 855–858.
- Hasanuzzaman M, Olabi. AG. 2016. Properties of Glass Materials. Reference Module in Materials Science and Materials Engineering. DOI: 10.1016/B978-0-12-803581-8.03998-9, pp 1-12.
- Henry GW, Eaton JA. 1995. Robotic telescopes: current capabilities, present developments, and future prospects for automated astronomy. 106th annual meeting of the Astronomical Society of the Pacific, Flagstaff, Arizona. *Astronomical Society of the Pacific*. Available at: <https://trove.nla.gov.au/work/21681638>. p 239.
- Howard NE. 1984. Handbook for Telescope Making. ISBN-10: 006181394X. pp 64-79
- Jinguan C, Humphries CM. 1982. Thin mirrors for large optical telescopes. *Vistas in Astronomy*. 26: 15–35.
- Laing RA. 1995. Control system for the William Herschel Telescope: performance and recent developments in Telescope Control Systems. Proceedings of SPIE. 2479: 41-49.
- Luc A. 1995. Optimized axial support topologies for thin telescope mirrors. *Optical Engineering* 34(2): 567-574
- Malacara D. 2007. Optical Shop Testing. A John Wiley & Sons. Inc. ISBN: 978-0-471-48404-2. pp 320-327.
- Melsheimer F, Genet RM. 1984. A Computerized Low-Cost 0.4-Meter Research Telescope. *International Amateur-Professional Photoelectric Photometry Communication* 15: 33-36.
- Mueller R, Hoeness H, Espiard J, Paseri J, Dierickx P. 1993. The 8.2-m primary mirrors of the VLT. *The Messenger* 73: 1–8.
- Nelson JE, Lubliner J, Mast TS. 1982. Telescope mirror supports: plate deflections on point supports. *Advanced Technology Optical Telescopes* 332(10) 212–228.
- Richard B. 1985. Build Your Own Telescope. Second English Edition. Willmann-Bell. ISBN: 0943396425. pp 240-150
- Rodriguez DJ, Martinez JJ, Berenguer C. 2017. Condition Monitoring of a Friction Drive. 3rd IEEE Colombian Conference on Automatic Control (CCAC 2017). pp 1-6.
- Schmalz, S, Molotov I, Voropeaev V, Krugly Y, Kauprianov V, Elenin L, Graziani F, Frofeev d, Kudak V, Wolf A. 2019. ISON S Sub-Network of small aperture telescopes for observations of NEOS, space debris and meteors. 1st NEO and Debris Detection Conference. ESA Space Safety Programme Office. pp 2-8.
- Scholze H. 1991. Properties of Glass. *Glass* 454:156–364.
- Smith HJ. 1989. A decade of cost-reduction in very large telescopes. *Astrophysics and Space Science* 160: 123–134.
- Tripurari SK, Ravi NB. 2013. Design and development of telescope control system and software for the 50/80 cm Schmidt telescope. *Optical Engineering* 52(8): 1-14.
- Van Breda IG, Culshaw B. 1990. Fibre-optic gyros as telescope attitude sensors. *Instrumentation in Astronomy VII* 1235: 448–458.
- Wang, G, Ma L, Yao Z, Li G. 2004. Experiment study on friction drive. *Astronomical Structures and Mechanisms Technology* 5495: 53-54.
- Wang G, Yang S, Wang, D. 2008. Error analysis of friction drive elements. *Advanced Optical and Mechanical Technologies in Telescopes and Instrumentation* 7018(B): 1-9. doi: 10.1117/12.791073
- Willstrop RV. 1995. New developments in telescope design. *Contemporary Physics* 36(6): 389–410.
- Wilson RN. 1999. Reflecting Telescope Optics II, Manufacture, Testing, Alignment Modern Techniques. ISBN 10: 3540603565. pp 169-199.